An appraisal of mesh quality measures for high-order curvilinear elements

January 14, 2024

Abstract

We present a review of *a priori* measures of high-order mesh quality and discuss a set of basic requirements they should meet. We then proceed to select a set of suitable candidates and appraised them according to criteria of sensitivity to distortion using a quadratic triangular element subject to motion of a mid-side node to investigate the variation of a quality measure. Finally we investigate what the "best" element shape is, according to the previous quality measures, when a curved boundary is imposed.

1 The role of the elemental mappings

The elemental mappings defining high-order curvilinear elements play a central role in quality metrics of the elemental shape. These are depicted in Figure 1. A high-order element is defined by the mapping, $\boldsymbol{\phi}_R$, between a *reference* element, Ω_R^e, defined in a parametric space of coordinates $\boldsymbol{\xi} = (\xi_1, \xi_2)$, and a *physical* element, Ω_P^e, with coordinates $\boldsymbol{x} = (x_1, x_2)$. Additionally, to evaluate elemental distortion, we introduce a mapping $\boldsymbol{\phi}$ between an *ideal* element, Ω_P^e, with coordinates $\boldsymbol{y} = (y_1, y_2)$ and the physical element. The mapping from the ideal to the physical element is then given by

$$\boldsymbol{\phi} = \boldsymbol{\phi}_I^{-1} \circ \boldsymbol{\phi}_P \tag{1.1}$$

Here the mapping $\boldsymbol{\phi}_P$ will be the isoparametric mapping that defines the high-order shape functions of the spectral/*hp* method [8][1].

The mappings $\boldsymbol{\phi}_P$, $\boldsymbol{\phi}_I$ and $\boldsymbol{\phi}$ are represented by their respective Jacobian matrices $\boldsymbol{J}_p$, $\boldsymbol{J}_I$ and $\boldsymbol{J}$, and their components are given by

$$[\boldsymbol{J}_P]_{ij} = \frac{\partial x_i}{\partial \xi_j}; \quad [\boldsymbol{J}_I]_{ij} = \frac{\partial y_i}{\partial \xi_j}; \quad [\boldsymbol{J}]_{ij} = \frac{\partial y_i}{\partial x_j} \tag{1.2}$$

In what follows, the mapping $\boldsymbol{\phi}$, its Jacobian matrix $\boldsymbol{J}$, with determinant $J = \det \boldsymbol{J}$, and its associated metric tensor $\boldsymbol{G} = \boldsymbol{J}\boldsymbol{J}^t$ with determinant $\det \boldsymbol{G} = J^2$

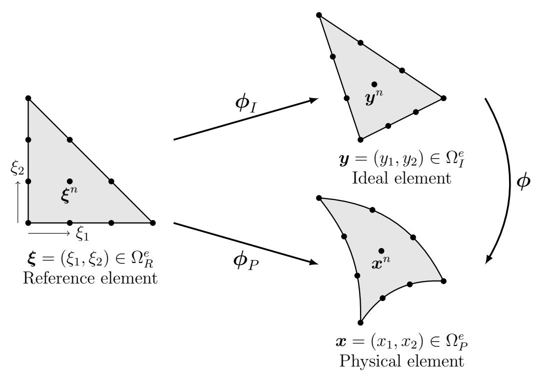

Figure 1: Notation used in defining the various mappings between the *physical*, *reference*, and *ideal* elements.

will permit the evaluation of changes in lengths, areas and angles, and will used to characterize, quantify and assess elemental distortions.

2 High-order mesh quality metrics

This section appraises several of the point-wise measures of high-order mesh quality proposed in the literature. These will be denoted by q_i.

A common measure of quality related to element distortion is the Jacobian of the mapping between the ideal and physical elements [3, 15]:

$$q_1 = J \tag{2.3}$$

The next quality measure, q_2, originates from the Laplacian mesh smoothing method [11] and is defined as

$$q_2 = \|\mathbf{J}\|_F = \mathrm{tr}(\mathbf{J}^T\mathbf{J}) \tag{2.4}$$

where $\|\cdot\|_F$ denotes the Frobenius norm.

An alternative quality measure q_3 can be obtained by considering the metric tensor [12, 11], namely

$$q_3 = \|\mathbf{G}\|_F \tag{2.5}$$

[1] These are implemented in the open-source code Nektar++: `www.nektar.info`.

Copyright © 2024
Copyright for this paper is retained by authors

The equal volume mesh quality measure, q_4, originates from the variational mesh generation method [2], which was designed by [11]. It is expressed as

$$q_4 = J^2 \tag{2.6}$$

A quality measure, q_5, that aims at favouring mesh orthogonality [6] is given by

$$q_5 = \|\mathrm{adj}(\mathbf{J})\|_F \tag{2.7}$$

where $\mathrm{adj}(\mathbf{J})$ denotes the adjoint of the Jacobian matrix.

Reference [5] proposed mesh quality measure, q_6, associated with harmonic maps:

$$q_6 = J \left\|\mathbf{J}^{-1}\right\|_F \tag{2.8}$$

Tinico-Ruiz and Barrera-Sánchez [16] have devised the aspect ratio mesh quality measure, q_7, given by

$$q_7 = \|\mathbf{J}\|_F / J \tag{2.9}$$

The shape mesh quality measure, q_8, minimizes geometric distortion of isoparametric elements [13], and is expressed using matrix norms [11] as

$$q_8 = \frac{3}{2} J^{-4/d} \left[\left\|\mathbf{J}^T\mathbf{J}\right\|_F - (1/3)\left\|\mathbf{J}\right\|_F^2\right] \tag{2.10}$$

where d is the dimension of the problem given.

Knupp [11] proposed two measures of distortion based on the Jacobian. The measure q_9, a non-dimensional version of q_6, given by

$$q_9 = J^{2/3} \left\|\mathbf{J}^{-1}\right\|_F \tag{2.11}$$

and the inverse mean ratio measure q_{10}, a non-dimensional version of q_7, given by

$$q_{10} = J^{-2/3} \left\|\mathbf{J}\right\|_F \tag{2.12}$$

Freitag and Knupp [14, 4, 10] have devised quality measures based on the condition number of the Jacobian matrix

$$q_{11} = \|\mathbf{J}\|_F \left\|\mathbf{J}^{-1}\right\|_F \tag{2.13}$$

and the metric tensor

$$q_{15} = \|\mathbf{G}\|_F \left\|\mathbf{G}^{-1}\right\|_F \tag{2.14}$$

Branets and Carey [1] proposed a shape distortion measure that aims to detect elemental distortions and control element size

$$q_{12} = \frac{1}{J}\left[\frac{1}{d}\mathrm{tr}(\mathbf{G})\right]^{d/2}, \tag{2.15}$$

an elemental dilation measure to control mesh gradation

$$q_{13} = \frac{1}{2}\left(\frac{V}{|\mathbf{J}|} + \frac{|\mathbf{J}|}{V}\right) \tag{2.16}$$

where V is the size of the target element, and a measure that is a linear combination of these two

$$q_{14} = (1-\alpha)q_{12} + \alpha q_{13} \tag{2.17}$$

with $0 \le \alpha \le 1$.

2.1 Appraisal of selected quality measures. To investigate the sensitivity of the quality measures to element distortion. we subject a quadratic triangular element to a symmetric deformation defined in terms of the coordinates (x_1, x_2) of a mid-side node only (Figure 2).

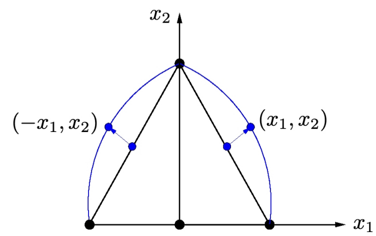

Figure 2: Symmetric distortion represented by the motion of a side node of coordinates (x_1, x_2).

We define an elemental measure of mesh quality, Q, from its values at a set of quadrature points on the reference element, $q(\boldsymbol{\xi}_i^q), i = 1 \ldots N_q$ where the number N_q of quadrature points, as

$$Q = \frac{\min_i \{q(\boldsymbol{\xi}_i^q);\ 1 \ldots N_q\}}{\max_i \{q(\boldsymbol{\xi}_i^q);\ 1 \ldots N_q\}} \tag{2.18}$$

We use a Gauss-Lobatto-Legendre quadrature rule [8] with $N_q = 3$ for a mesh with polynomial order $P = 2$. Contours maps of Q are shown for all the selected measures $Q_1, \ldots Q_{14}$ and Q_{15} in Figure 3.

All the quality measures reach a maximum value that corresponds to the straight-sided element, as expected. A number of measures exhibit very similar behaviour, namely the sets: $\{Q_1, Q_4\}$, $\{Q_2, Q_3, Q_5\}$, and $\{Q_6, Q_7, Q_9, Q_{10}, Q_{11}, Q_{12}\}$, thus reducing the number of potential candidates. Measure Q_1 is preferred to Q_4 due to the presence of multiple local extrema in Q_4. Measure Q_3 is favoured due to being steeper near the maximum. We select Q_6 from the other similar measures in this set. Quality measures Q_{13} and Q_{14} are discarded because they are not convex and also exhibit several local extrema. The final set of measures is $\{Q_1, Q_3, Q_6, Q_8, Q_{15}\}$. The following section will assess their sensitivity to boundary displacements.

Copyright © 2024
Copyright for this paper is retained by authors

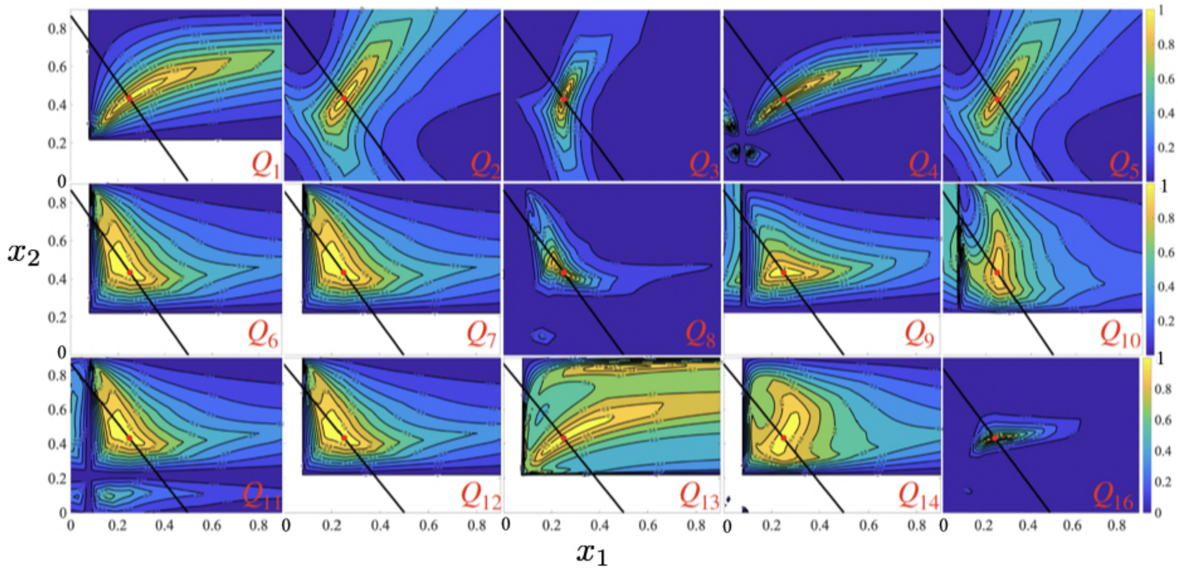

Figure 3: Contour maps and level sets of the value of the selected quality measures Q_i.

3 Mesh quality near boundaries

To determine the best shape of a curvilinear element with a side on the boundary, we consider a quadratic straight-sided equilateral triangle where a mid-side node is displaced along a symmetry axis a distance δ to incorporate boundary curvature, as depicted in Figure 4.

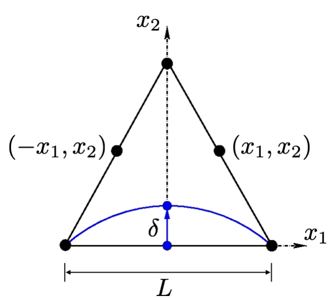

Figure 4: A quadratic element with a curved side on the boundary. The displacement δ of the mid-side node controls its curvature.

The variation of the selected quality metrics, Q_i, with the displacement of the mid-point of the boundary side, δ/L, is shown in Figure 5. Note that the Jacobian is zero for $\delta/L = \sqrt{3}/4$.

All the measures decrease monotonically with increasing displacement δ, but Q_6 becomes singular at the point where $J = 0$. The decrease of measure Q_1 with δ is the slowest, and takes negative values. The others are always positive and differ in their rate of decrease which is the fastest for measures Q_8 and Q_{16}.

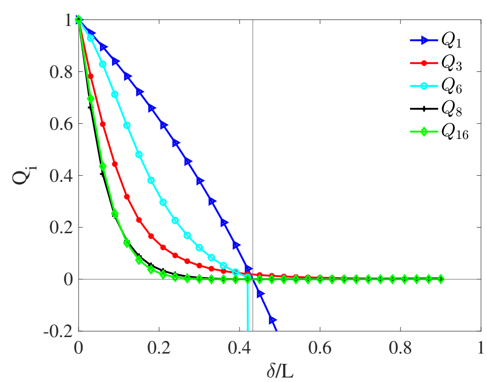

Figure 5: Variation of $\{Q_1, Q_3, Q_6, Q_8, Q_{15}\}$ with δ.

3.1 What is the "best" element shape? The problem of finding the best shape of an element for quality measure Q_i is reduced to that of finding the values of the location (x_1, x_2) that maximizes $Q_i(x_1, x_2)$ for a given δ. We use Brent's principal-axis method PRAXIS optimization without derivatives implemented in the code NLopt [7]. The stopping criteria is that the distance between consecutive iterations of the optimal point is smaller than 10^{-6}. The coordinates of the optimal locations leading to the best elemental shape are displayed in Figure 6 in which the curves represent the motion of the optimal point as the displacement δ increases.

The location of the optimal point for $\delta = 0$ is the same for all the measures as expected, but it differs

Copyright © 2024
Copyright for this paper is retained by authors

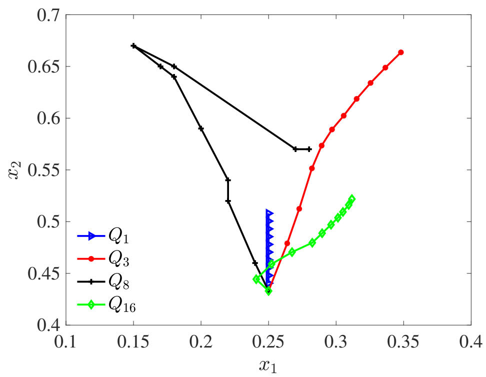

Figure 6: Coordinates of the mid-side node of the modified element leading to optimal quality, i.e. the best element shape, for the selected quality metrics.

significantly for values $\delta > 0$. The variation along the curves is smooth for all the measures except Q_8 that exhibits erratic behaviour as it exhibits local extrema for larger values of δ and fails to converge to the global maximum. As a results the curve for Q_8 in Figure 6 as been obtained using uniform sampling of the values of Q_8 to locate the global maximum.

Measures Q_3 and Q_{15} are better behaved, but Q_{15} shows slight discrepancies in the early stages of the displacement. The behaviour for the measure Q_1 is unexpected as the mid-side node moves vertically according to the optimum location.

A final illustration of the element shapes obtained through the optimization of the mesh quality is included in Figure 7 which shows the "best" shapes for the measures $\{Q_1, Q_3, Q_8, Q_{15}\}$ with different displacements $\delta/L = \{0.1, 0.2, 0.3\}$. These measures differ significantly in their sensitivity to boundary displacements. The measures Q_1 and Q_8 appears to be the less sensitive whilst the largest element distortion occurs for measure Q_3 that seems to produce largely inflated shapes. Measure Q_{15} exhibits a moderate sensitivity to displacements that leads to a smoother variation of the shape as the boundary displacement increases.

4 Conclusions and further remarks

We have carried out two test to assess a set of high-order mesh quality measures based on their sensitivity to elemental distortion from a straight-sided element.

The first test monitored the variation of the quality of a quadratic triangular element subject to the motion of a side node. All the measures attained a maximum value for the straight-sided triangle as expected, but some of them produced multiple local extrema which made them unsuitable for optimization.

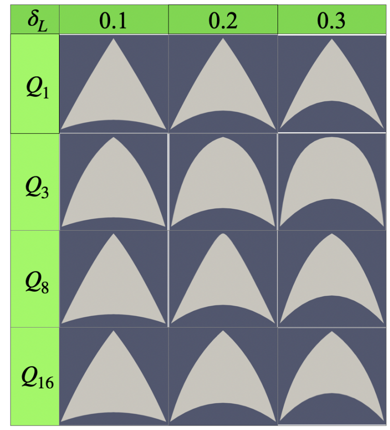

Figure 7: "Best" element shapes obtained for mesh quality measures Q_1, Q_3, Q_8 and Q_{16} with different displacements $\delta/L = \{0.1, 0.2, 0.3\}$.

This reduced the set of suitable candidates to the measures $\{Q_1, Q_3, Q_8, Q_{15}\}$.

The second test aims at obtaining the "best" shape of an element subject to a boundary displacement according to the set of quality measures selected in the previous step. This was achieved via an derivative-free optimization procedure. The analysis of this test showed that measure Q_1 exhibited unexpected behaviour but produced reasonably shaped elements, measure Q_8 developed additional local extrema that caused difficulties to the optimizer, and measures Q_3 and Q_{15} produced a smooth response to boundary displacement, but measure Q_3 allowed for severely distorted, possibly invalid elements for large displacements.

The main conclusion of this analysis is that the measure Q_6 verifies all the requirements set out in the two tests.

Acknowledgements

This project has received funding from the European Union's Horizon 2020 research and innovation programme under the Marie Skłodowska-Curie grant agreement No 955923.

This work started and expands from a preliminary analysis of high-order mesh quality carried out by Dr Ümit Keskin in his PhD thesis [9]. His initial contribution is greatly acknowledged.

References

[1] L. Branets and G.F. Carey. Condition number bounds and mesh quality. *Numer. Linear Algebra Appl.*, 17:855–869, 2010.

Copyright © 2024
Copyright for this paper is retained by authors

[2] K.Y. Szema C.L. Chen and S.R. Chakravarthy. Optimization of unstructured grid. In *33^{rd} Aerospace Sciences Meeting and Exhibit*, number AIAA 95-0217, Reno, NV, USA, January 1995. AIAA.

[3] S. Dey, R.M. O'Bara, and M.S. Shephard. Curvilinear mesh generation in 3D. In *Proceedings of the 8^{th} International Meshing Roundtable*, pages 407–417, South Lake Tahoe, CA, USA, October 1999.

[4] L.A. Freitag and P.M. Knupp. Tetrahedral mesh improvement via optimization of the element condition number. *Int. J. Num. Meth. Eng.*, 53:1377–1391, 2002.

[5] J. Brackbill and J. Saltzman. Adaptive zoning for singular problems in two dimensions. *Journal of Computational Physics*, 46:342–368, 1982.

[6] Olivier-Pierre Jacquotte and Jean Cabello. A variational method for the optimization and adaptation of grids in computational fluid dynamics. *NASA STI/Recon Technical Report A*, 1988:31830, 1988.

[7] Steven G. Johnson. The NLopt nonlinear-optimization package. `https://github.com/stevengj/nlopt`, 2007.

[8] G.E. Karniadakis and S.J. Sherwin. *Spectral/hp Element Methods for CFD.* Oxford University Press, 1999.

[9] Ümit Keskin. *Addressing some current issues in linear and high-order meshing.* PhD thesis, Imperial College London, 2014.

[10] P. Knupp. Matrix norms & the condition number: A general framework to improve mesh quality via node-movement. In *Proceedings of the 8^{th} International Meshing Roundtable*, pages 13–22, South Lake Tahoe, CA, USA, October 1999. Springer-Verlag.

[11] Patrick M. Knupp. Algebraic mesh quality metrics. *SIAM Journal on Scientific Computing*, 23(1):193–218, January 2001.

[12] G. Liao. Variational approach to grid generation. *Numerical Methods for Partial Differential Equations*, 8:143–147, 1992.

[13] A. Oddy, J. Goldak, M. McDill, and M. Bibby. A distortion metric for isoparametric elements. *Trans. Canad. Soc. Mech. Engrg.*, 12:213–217, 1988.

[14] P. Knupp. Achieving finite element mesh quality via optimization of the Jacobian matrix norm and associated quantities. Part II: A framework for volume mesh optimization. *Internat. J. Numer. Methods Engrg.*, 48:1165–1185, 2000.

[15] S.J. Sherwin and J. Peiró. Mesh generation in curvilinear domains using high-order elements. *Int. J. Numer. Meth. Engng.*, 53:207–223, 2002.

[16] J.G. Tinico-Ruiz and P. Barrera-Sánchez. Smooth and convex grid generation over general plane regions. *Mathematics and Computers in Simulation*, 46:87–102, 1998.

Copyright © 2024
Copyright for this paper is retained by authors